Modeling of Chemical Equilibrium and Gas Phase Behavior for the Direct Synthesis of Dimethyl Carbonate from CO2 and Methanol

4 AUTHORS, INCLUDING:

Felipe Bustamante
University of Antioquia
30 PUBLICATIONS **447** CITATIONS

SEE PROFILE

Aída Luz Villa
University of Antioquia
54 PUBLICATIONS **318** CITATIONS

SEE PROFILE

Modeling of Chemical Equilibrium and Gas Phase Behavior for the Direct Synthesis of Dimethyl Carbonate from CO_2 and Methanol

Felipe Bustamante,* Andrés F. Orrego, Sebastián Villegas, and Aída L. Villa

Environmental Catalysis Research Group, Sede de Investigación Universitaria SIU, Universidad de Antioquia, Medellín, Colombia

Ⓢ *Supporting Information*

ABSTRACT: The chemical and gas phase equilibrium of the direct synthesis of dimethyl carbonate (DMC) from methanol (MeOH) and CO_2 was modeled under mild conditions of temperature and pressure. Deviations from ideality for the quaternary mixture (CO_2 + MeOH + DMC + H_2O) were estimated using the $\gamma - \phi$ thermodynamic approach. Binary interaction parameters (k_{ij}) and UNIQUAC parameters (A_{ij}) were extracted from VLE data reported in the literature. The results show that MeOH conversion is enhanced by increasing the pressure and reducing the temperature; however, pressure and temperature are bounded by the dew point. Data of P, T, and vapor compositions obtained from modeling chemical equilibrium were used to predict dew points of the reacting mixture and to establish the region of T and P where the gas-phase reaction could be carried out. To avoid condensation, an increase in pressure must be accompanied by a temperature increase. Moreover, the larger the methanol concentration in the feed mixture is, the higher is the required temperature.

■ INTRODUCTION

The interest in the production of dimethyl carbonate (DMC), a compound cataloged as a "green chemical", has been growing over the past decade. DMC is an environmentally friendly raw material of wide versatility as well as a possible substitute of highly corrosive or toxic reagents in organic synthesis, such as dimethyl sulfate, chloromethane, and phosgene. Moreover, DMC can act as a methylating and carbonylating agent or as an intermediate in the production of higher carbonates, polyurethanes, isocyanates, polycarbonates, and other fine chemicals.[1] Furthermore, due to its high oxygen content and reduced environmental impact, DMC has also emerged as a potential substitute for methyl tertiary butyl ether (MTBE), used as an oxygenating fuel additive (i.e., octane enhancer).[2]

The direct synthesis of DMC from methanol (MeOH) and carbon dioxide (CO_2), reaction I, is an attractive route to replace the traditional synthesis via phosgenation of MeOH.[3]

$$2CH_3OH + CO_2 \rightleftharpoons (CH_3O)_2CO + H_2O \qquad (I)$$
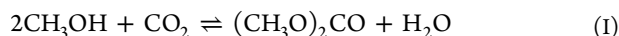
Several catalysts have been reported for the one-step synthesis of DMC:[4−7] organometallic compounds based on Sn(IV) such as n-R$_2$Sn(OMe)$_2$ (R = Me, Bu),[8] series of n-butyl(alkoxy) stannanes,[9−12] decakis(diorganotin(IV)) oxoclusters[13] and immobilized[14−16] were applied successfully where DMC yield reported was between 30 and 88% in these systems. The high performance had been partly attributed to the fact that reaction I becomes thermodynamically favorable as the system pressure increases, such as described by Cai et al.[17] and Leino et al.[6] in theoretical studies of the dependence of ΔG_{rxn} with pressure. Some strategies as the in situ water remotion from reaction system or the inclusion of coupled reactions have been addressed for overcoming thermodynamic limitations. In this way, the reaction had also been carried out in the presence of dehydrates, additives, or promoters such as ortho esters,[18,19] acetals,[20] 2,2-dimethoxypropane,[21] or molecular sieves[22] to minimize the water concentration in the reaction system.

Ni(CH$_3$COO)$_2$,[23−25] carbodiimides,[26] tantalum alkoxides,[27] and niobium complexes[28−30] also catalyze the reaction; nevertheless, almost all previous catalytic experiments have been reported in the liquid phase and/or under high pressure conditions (supercritical conditions) showing disadvantages related with high cost of the starting materials, the difficulty in the catalyst-product separation due to the homogeneous nature of the catalyst and rapid catalyst deactivation.

On the other hand, basic heterogeneous catalysts (K_2CO_3, CH_3OK, KOH),[17,19,31−34] solid acid−base catalysts such as zirconia,[35,36] and modified zirconia by ceria[37−41] or acidic compounds $H_3PW_{12}O_4$−ZrO_2[42] or phosphoric acid H_3PO_4−ZrO_2[43,44] or ZrO_2−KCl[45] promote catalytic activity. Heteropoly acids ($H_3PW_{12}O_{40}$−$Ce_xTi_{1-x}O_2$ and $H_3PW_{12}O_{40}$−$Ce_xZr_{1-x}O_2$),[46−48] CeO_2,[49] Al_2O_3−CeO_2,[50] Ga_2O_3/$Ce_xZr_{1-x}O_2$,[51] metal oxide−$Ce_{0.6}Zr_{0.4}O_2$,[52] ZrO_2−MgO,[53] ZrO_2/SiO_2, and SnO_2/SiO_2[54] are also active materials for the DMC formation from methanol and CO_2. In this group of catalysts, the reaction was carried out at pressures above 4 MPa, and similarly to that using homogeneous catalysts, batch operations at high pressure can increase operational cost in the process when pumping and compression to elevated pressure or thick walled vessels for high pressure are required. Nevertheless, a gas-phase process carried out at moderate conditions would greatly facilitate process control, catalyst recovery, and would reduce both operational and capital costs.

Few catalytic studies have been reported in batch operation at low pressure (0.12−0.5 MPa), where catalysts such as $Cu_{1.5}PMo_{12}O_{40}$,[55] CeO_2 with acetonitrile as dehydrate[56] and heteropolyoxometalates[57,58] have been probed but without a

significantly increase of DMC yield compared with gas-phase reaction in continuous reaction system.

Heterogeneous catalysts reported for gas-phase synthesis, Ni−Cu/MoSiO(VSiO),[59] Cu−KF/MgSiO,[60] H_3PO_4−V_2O_5,[61] Cu−Ni/VSO,[62] Cu−(Ni,V,O)/SiO_2 with photoassistance,[63] Cu−Ni/C[64] (C = graphite,[65] MWCNTs,[66] AC,[67] TEG,[68] graphite oxide,[69] GNS[70]), Rh/ZSM-5,[71] $CuCl_2$/AC,[72] $Co_{1.5}PW_{12}O_{40}$[73] and Cu−Ni/diatomite[74] in which the reaction was carried out at low pressure (0.1−1.2 MPa), moderate temperatures (353−500 K) and continuous flow, seem less productive compared to the homogeneous reaction. These studies have remarked that DMC obtained from reaction I is drastically limited by the chemical equilibrium leading to very low DMC yields partly due to the low methanol conversion at equilibrium,[18,35,75] but no deep studies about the limit of MeOH conversion had been done.

Zhao et al.[76] presented a first approach to estimate the gas-phase equilibrium conversion considering ideal-gas behavior. Moreover, Zhao and co-workers made some assumptions in the estimation of thermodynamic data which are not accurate, that is, in calculating the entropy of DMC they used the group CO−(O)(C), which is not present in DMC, instead of the group CO−(O)(O) and did not consider the possible partial condensation of the reaction mixture at equilibrium conditions. Thence, the calculated gas-phase equilibrium conversion may differ significantly from the actual value. An accurate description of the equilibrium conversion is the starting point to improve carbonate yield in a continuous or semicontinuous process where water vapor is removed from the reactor, for example, by a coupling of reaction and separation through membranes in a catalytic membrane reactor (CMR). Taking into consideration that this approach will be facilitated if the reaction is conducted in the gas phase, this study presents a more accurate modeling of chemical equilibrium in order to theoretically determine the best conditions (temperature, pressure, and feed composition) to conduct the gas-phase reaction at (or close to) equilibrium conversion. Specifically, the nonideality of the mixture is considered, and the limits of temperature and pressure to prevent partial condensation are evaluated. As a result of integrating the chemical equilibrium model and gas phase behavior, which have been studied independently, we report the equilibrium dew pressure assuming a single reaction (reaction I) in the gas phase.

■ METHODOLOGY

Thermodynamic Data. Thermodynamic data of CO_2, MeOH, and H_2O are already available.[77] However, this is not the case for DMC. Therefore, the gas phase standard free energy (Gibb's function) and heat capacity for DMC were estimated with Benson's group contribution method.[78] Estimation of the standard thermodynamic properties of ideal gases by Benson's method has shown good agreement with experimental values for a large number of organic molecules, and gives lower deviations compared with other methods reported in the literature.[78] Thermodynamic data of the species involved in this study, including DMC (see calculations below), are shown in Table 1.

Standard Free Energy Calculation (ΔG_f^0) for DMC. $\Delta H_{f,298K}^0$ of DMC as ideal gas was estimated from its constituent groups using $\Delta H_{f,k,298K}^0$ group contribution values reported by Steele et al.,[79] giving a value of 571.0 kJ mol^{-1} (see Table 2).

Table 1. Thermodynamic Data of Pure Substances Involved in the Direct Synthesis of DMC[77]

	gas			
species	ΔH_f^0 (kJ mol^{-1})	ΔG_f^0 (kJ mol^{-1})	S^0 (J mol^{-1} K)	C_{P_1} (J mol^{-1} K)^a
methanol	−201	−162.3	239.9	44.1
carbon dioxide	−393.51	−394.38	213.8	37.1
water	−241.8	−228.6	188.8	33.6
DMC	−571.0	−466.85^b	366.01^b	128.12^{b,c}

^{a}Between 273 and 433 K. ^{b}Estimated in this work by Benson group contribution. ^{c}Average between C_p (298 K) and C_p (500 K).

Table 2. Heat of Formation of DMC by Benson's Method

Benson's group	number of groups N_k	group contribution^a $\Delta H_{f,k}^0$ (kJ mol^{-1})	total
CH_3−(O)	2	−42.4	−84.8
O−(CO)(C)	2	−179.71	−359.4
CO−(O)(O)	1	−126.8	−126.8

^{a}Values reported by Steele et al.[79]

The experimental value reported by Steele and co-workers for the contribution of CO−(O)(O) group to the enthalpy of formation of DMC (−126.8 kJ mol^{-1}) is very close to the value estimated from computational chemistry simulations (−125.7 kJ mol^{-1}) by Khan et al.[80] The error associated to ΔH_f^0 is around 0.05%. Therefore, in order to estimate the ideal-gas standard free energy and ideal-gas heat capacity of DMC, the entropy value for CO−(O)(O) group contribution reported by Khan et al.[80] was considered.

The estimation of standard molar entropy (S_{298K}^0) depends not only on the constituent groups (S_k^0), but also on molecular symmetry, associated to S_s^0 term in eq 1.

$$S^0(298 \text{ K}) = \sum_k N_k(S_k^0) + S_s^0 \tag{1}$$

This symmetry entropy, S_s^0, is independent of temperature and given by eq 2.

$$S_s^0 = R \ln(N_{oi}) - R \ln(N_{ts}) \tag{2}$$

where N_{oi} is the number of optical isomers of the molecule, being 1 if the molecule has no optical isomers, which is the case with DMC; N_{ts} is the total symmetry number, being 18 for DMC. More details on how to obtain N_{ts} values are given by Poling et al.[78] Finally, $\Delta G_{f,298K}^0$ is calculated by means of eq 3 and eq 4.

$$\Delta G_f^0(298K) = \Delta H_f^0(298K) - 298K[S^0(298K) - S_{el}^0(298K)] \tag{3}$$

where

$$S_{el}^0 = \sum_e N_e(S_e^0) \tag{4}$$

Values of $\Delta H_{f,k}^0$, S_k^0, $C_{p,k}^0$ for each group and S_e^0 for elements are listed Table 3.

From the group contribution data listed in Table 3, the estimated value of ΔG_f^0 (298K) for DMC as ideal-gas is −466.85 kJ mol^{-1}.

The gas phase ΔH_{rxn}^0 and ΔG_{rxn}^0 of reaction I at 298 K, calculated from the stoichiometric numbers and the heat and

Table 3. Group Contributions[78]

group (k)	$\Delta H^0_{f,k}$ 298 K	S^0_k 298 K	$C^0_{p,k}$		
			298 K	400 K	500 K
$CH_3-(O)$	−42.19	127.1	25.87	32.80	39.35
$O-(CO)(C)$	−180.41	35.12	11.64	15.86	18.33
$CO-(O)(O)^a$	−125.68	65.6	27.73	32.34	36.48
element (e)	N_e	S^0_e			
C	3	6			
H_2	3	130			
O_2	3/2	205			

^{a}Values for $CO-(O)(O)$ reported by Khan et al.[80]

Gibbs free energy of formation of reactants and products, are −17.29 and 23.53 kJ mol^{-1}, respectively. These values indicate that the gas phase reaction is exothermic and nonspontaneous at room temperature (298 K).

To obtain ΔH^0_{rxn} and ΔG^0_{rxn} at different temperatures, data of molar ideal-gas heat capacities, C^0_p, were used. For DMC a cubic correlation was used to fit the data estimated by Benson's method between 298 and 500 K. Then an expression for the Gibbs free energy change of the reaction as a function of temperature was obtained by combining the Gibbs−Helmholtz equation with Kirchoff's law.[81] Finally, the equilibrium constant K was calculated from the Gibbs free energy at each temperature.

Chemical Equilibrium Modeling. The effects of the initial concentration of MeOH, pressure, and CO_2/MeOH feed ratio on equilibrium conversion in the temperature range between 298 and 433 K were analyzed. For the direct synthesis of DMC, equilibrium conversion can be related to the equilibrium constant as shown in eq 5:

$$K_{eq}(T) = \frac{a_{DMC}a_{H_2O}}{a^2_{MeOH}a_{CO_2}}$$

$$= \frac{\frac{1}{4}X^2_{eq}(1 - 0.5y_{MeOH,0}X_{eq})}{y_{MeOH,0}(1 - X_{eq})^2\left(\Theta_{CO_2} - \frac{1}{2}X_{eq}\right)}$$
$$\times \left(\frac{\bar{\phi}_{DMC}\bar{\phi}_{H_2O}}{(\bar{\phi}_{MeOH})^2\bar{\phi}_{CO_2}}\right)_{eq}\left(\frac{(\phi^0_{MeOH})^2\phi^0_{CO_2}}{\phi^0_{DMC}\phi^0_{H_2O}}\right)_{eq}\left(\frac{P^0}{P}\right)$$

(5)

where $\Theta_{CO_2} = y_{CO_2,0}/y_{MeOH,0}$.

Fluid Phase Equilibria Modeling. Because this work is concerned with liquid−vapor equilibria at low and moderate pressures, we have used the $\gamma - \phi$ approach (activity coefficient for the liquid phase; fugacity coefficient for the vapor phase) in order to evaluate dew points at P, T and molar compositions in gas phase derived from chemical equilibrium model. Previous reports[82,83] showed that both Soave−Redlich−Kwong equation of state (SRK EoS)[84] with the Huron and Vidal mixing rules[85] modified by Michelsen[86] (MHV2), and Peng−Robinson−Stryjek−Vera equation of state (PRSV EoS)[87] with the van der Waals one-fluid (1PVDW) mixing rules,[78,88] reasonably predict VLE of different binary subsystems from the quaternary CO_2−MeOH−H_2O−DMC mixture at high and low pressures. Since an analysis at moderate pressures is considered in this work, PRSV−1PVDW EoS was selected to describe the gas phase behavior. Moreover, Piñero et al.[83] reported the binary interaction parameters as a function of temperature, allowing

extrapolation, within certain limits, to higher temperatures and prediction of the vapor behavior at different reaction conditions. UNIQUAC[89,90] model was considered for calculating activity coefficients in the liquid phase; parameters were taken from the literature.[82,91,92]

■ RESULTS AND DISCUSSION

Validation of Fluid Phase Equilibria Modeling Approach. *Binary Subsystems.* A review of experimental dew points ($P−y$ data) has been made by selecting results from binary systems at low or moderate pressure.[82,92−99] Experimental dew points for the different binary systems were then compared with those calculated using the $\gamma - \phi$ approach with binary interaction parameters listed in Table 4 and Table 5; the

Table 4. Temperature Dependence of Binary Interaction Parameters k_{ij} and l_{ij}[79]

	k_{ij}	l_{ij}	T (K)
CO_2 (1) + methanol (2)	$k_{12} = -0.04889 + 0.000142T$	$l_{12} = 0.11655 - 0.00049T$	298 to 313
	$k_{21} = -0.32186 + 0.001202T$	$l_{21} = 0.0034067 - 3 \times 10^{-5}T$	
CO_2 (1) + water (2)	$k_{12} = 3.06296 - 0.009680T$	$l_{12} = 0$	323 to 353
	$k_{21} = -0.35981 + 0.000859T$	$l_{21} = 0$	
CO_2 (1) + DMC (2)	$k_{12} = -0.00432 + 0.000010T$	$l_{12} = 8.2567 \times 10^{-5} + 1.47 \times 10^{-6}T$	310 to 330
	$k_{21} = -0.03110 + 0.000080T$	$l_{21} = 0.0002787 - 2.67 \times 10^{-6}T$	
methanol (1) + water (2)	$k_{12} = -0.61880 + 0.001570T$	$l_{12} = 0$	313 to 333
	$k_{21} = -0.39211 + 0.000815T$	$l_{21} = 0$	
DMC (1) + methanol (2)	$k_{12} = -0.03545 + 0.000282T$	$l_{12} = 0$	313 to 358
	$k_{21} = 0.03595 - 0.000035T$	$l_{21} = 0$	
DMC (1) + water (2)^a	$k_{12} = -0.34043$	$l_{12} = -9.22 \times 10^{-5}$	370 to 350
	$k_{21} = -0.0796$	$l_{21} = 1.942 \times 10^{-4}$	

^{a}Interaction parameters for the low DMC concentration side of the eutectic point.

results are shown in Figure 1 to Figure 6. The calculation routine was developed using MATLAB R2008b; the average

Table 5. Reported UNIQUAC Binary Interaction Parameters[82]

i	j	A_{ij} (cal mol^{-1})	A_{ji} (cal mol^{-1})
CO_2	methanol	502.12	131.709
CO_2	water	1546.5	994.997
CO_2	DMC	$-4971.1 + 22.49T^a$	$-2893.6 + 8.89T^a$
methanol	water	781.604	−435.901
methanol	DMC	$1033.29 - 2.78T^b$	$-1878.06 + 5.99T^b$
DMC	water	817.58^c	114.42^c

^{a}Estimated in this work by fitting with ASPEN Plus V7.3 software. ^{b}Values reported by Ma et al.[91] ^{c}Values reported by J. de la Torre et al.[92]
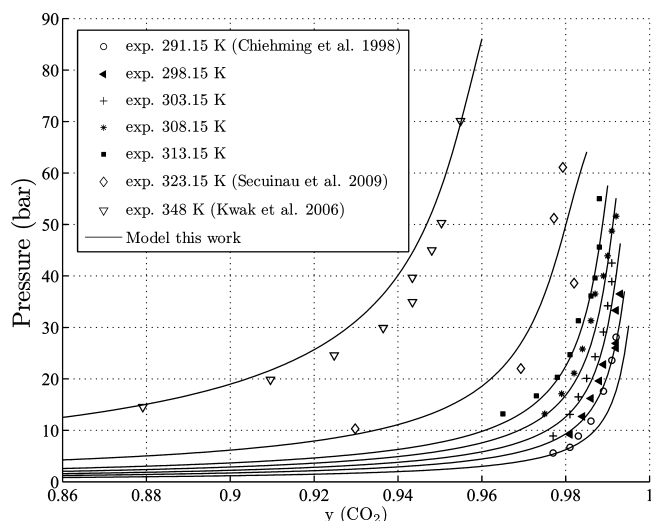
Figure 1. Experimental (points) and calculated (solid lines) P−y profiles for the CO_2−MeOH system at different temperatures. The AAD for P ranged from 7.6% (313.15 K) to 19% (291.15 K), whereas the AAD for y was below 0.5% (see the table in Supporting Information).
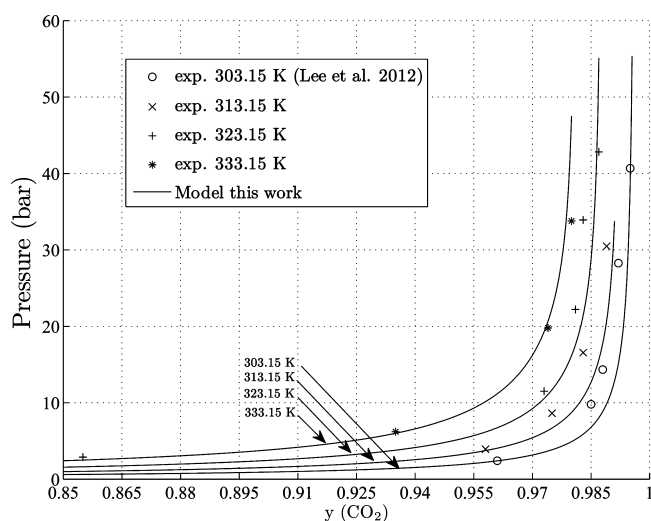

Figure 2. Experimental (points) and calculated (solid lines) P−y profiles for the CO_2−DMC system at different temperatures. The AAD for P ranged from 23.5% (313.15 K) to 26.6% (333.15 K), whereas the AAD for y was below 0.3% (see the table in Supporting Information).

absolute deviations (AAD%) for pressure and vapor phase composition are defined as:

$$\frac{\Delta P}{P} = \frac{1}{n} \sum_{i=1}^{n} \left[\frac{P_i^{exp} - P_i^{cal}}{P_i^{exp}} \right] 100$$

$$\frac{\Delta y}{y} = \frac{1}{n} \sum_{i=1}^{n} \left[\frac{y_i^{exp} - y_i^{cal}}{y_i^{exp}} \right] 100 \quad (6)$$

where n is the number of experimental data points and the superscripts exp and cal, represent experimental and calculated pressure and vapor composition values, respectively. The results indicate that the $\gamma - \phi$ method can reproduce experimental dew points with deviations below 5% for vapor composition. As can be observed from Figure 1 to Figure 6, the
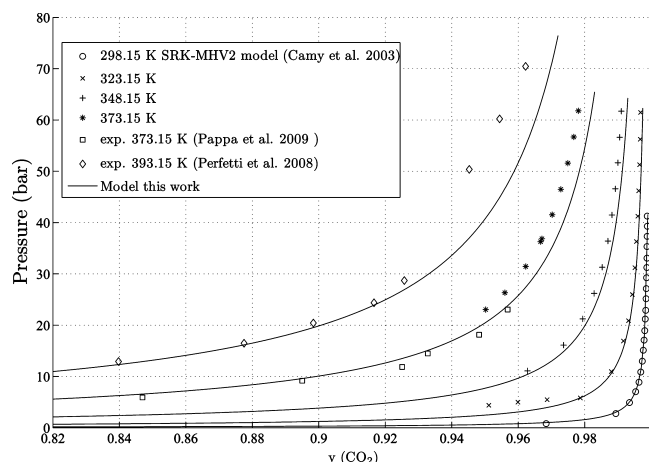

Figure 3. Experimental (points) and calculated (solid lines) P−y profiles for the CO_2−H_2O system at different temperatures. The AAD for P ranged from 9.4% (393.15 K) to 25.9% (298.15 K), whereas the AAD for y was below 0.8% (see the table in Supporting Information).
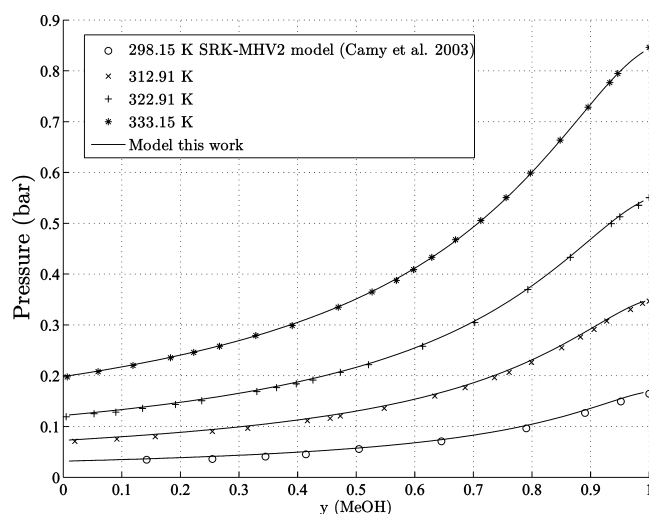

Figure 4. Experimental (points) and calculated (solid lines) P−y profiles for the MeOH−H_2O system at different temperatures. The AAD for P ranged from 0.3% (333.15 K) to 6.9% (298.15 K), whereas the AAD for y ranged from 1.1% (298.15 K) to 14.7% (333.15 K) (see the table in Supporting Information).

agreement is quite satisfactory, even though some discrepancies occur as noted below.

Experimental and calculated P−y profiles for the CO_2−MeOH system at different temperatures are shown in Figure 1; a good agreement with the experimental data at intermediate temperatures (298−313 K) can be observed. However, slight deviations occur at 291.15, 323.15, and 348.15 K. On the other hand, as shown in Figure 2 the predictions for the CO_2−DMC system are not quite as good. The deviations become more relevant as the temperature increases. The largest average absolute deviation for pressure is 26.6% at 333.15 K. These deviations are likely caused by the fact that the proposed model cannot satisfactorily represent this binary system. Indeed, according to previous studies[96,100] the $\phi - \phi$ approach would be more appropriate. For other binary subsystems, the model proposed in this work predicts well the experimental data. However, it is expected that the impact of the possible deviations in the estimation of the CO_2−DMC on the
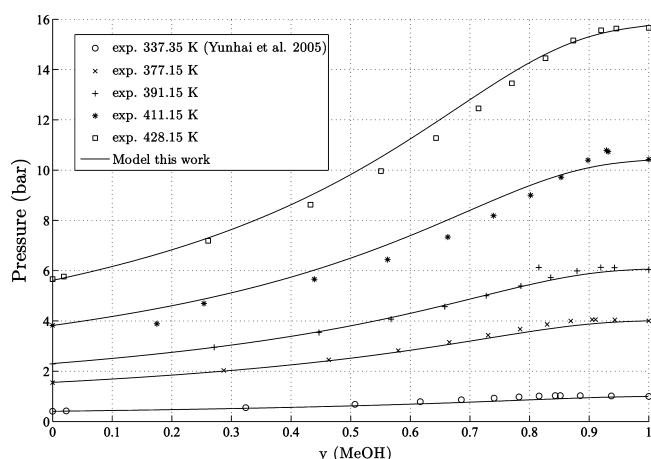
Figure 5. Experimental (points) and calculated (solid lines) $P-y$ profiles for the MeOH–DMC system at different temperatures. The AAD for P ranged from 1.5% (391.15 K) to 7.6% (337.35 K), whereas the AAD for y ranged from 2.0% (391.15 K) to 23.7% (337.35 K) (see the table in Supporting Information).
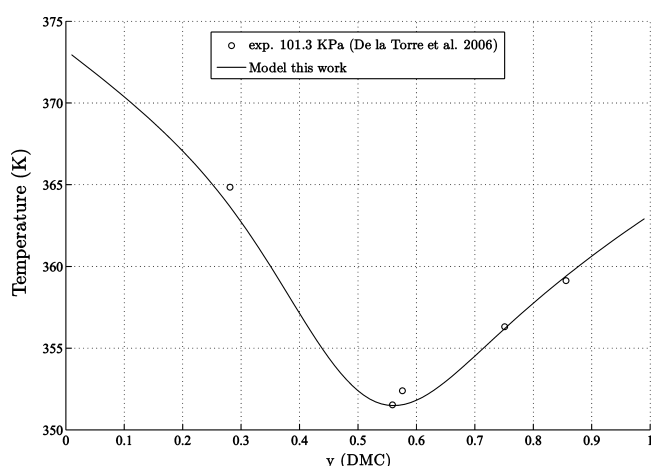

Figure 6. Experimental (points) and calculated (solid line) $T-y$ profiles for the DMC–H$_2$O system at 101.3 kPa. The AAD for T was 0.1% and the AAD for y was 4.2% (see the table in Supporting Information).

simulation of the quaternary mixture will be unimportant since, as it will be shown below, the equilibrium conversion of methanol achieved in the reaction is low, therefore the concentration of DMC will be very small compared to that of methanol or CO$_2$ which would exert a larger influence on the behavior of the quaternary system. The ability of the model to predict the CO$_2$–H$_2$O system, Figure 3, is very good, considering all range of temperatures (298.15–393.15 K) and CO$_2$ vapor concentration (0.84–1) used for the fitting. At higher temperatures some deviations are observed. Note that subsystems involving CO$_2$, can only be correlated with experimental data at pressures below 70 bar because the $\gamma - \phi$ method fails to describe the phase behavior of binary mixtures near the critical region. As several authors have reported for similar subsystems,[93−95,101−104] the $\phi - \phi$ model is more appropriate for evaluating the phase behavior at higher pressures.

In the range of temperature and pressure where the model was evaluated for CO$_2$–MeOH, CO$_2$–H$_2$O, and CO$_2$–DMC binary subsystems, CO$_2$ predominates in the vapor phase

(more than 80% mol), suggesting that CO$_2$ and condensable vapors could be recovered and recycled if the direct synthesis of DMC would be carried out in a continuous process.

The accuracy of the dew points calculated for the MeOH–H$_2$O subsystem, Figure 4, is very good with pressure AAD < 7% for all temperatures simulated; similar good agreement have been reported when the system was simulated with SRK–MHV2 model.[82]

Regarding the MeOH–DMC system, Figure 5, small deviations between experimental and predicted results, mainly at high temperatures and high MeOH concentrations, are observed. However, results for this system are quite satisfactory, with pressure AAD less than 7.6%.

In the DMC–H$_2$O system, Figure 6, the available $P-y$ experimental data is reproduced with satisfactory accuracy. A small deviation to the left of the eutectic point is observed. Nevertheless, the calculated eutectic point matches up correctly with that measured by J. de la Torre et al.[92]

Ternary Subsystem. Because the aim of the thermodynamic model is to predict the dew point of the quaternary reaction mixture, the accuracy of the model was tested against data of the ternary system CO$_2$–MeOH–DMC at 10 bar and 313 K reported by Piñero et al.[83] As shown in Figure 7, there is good
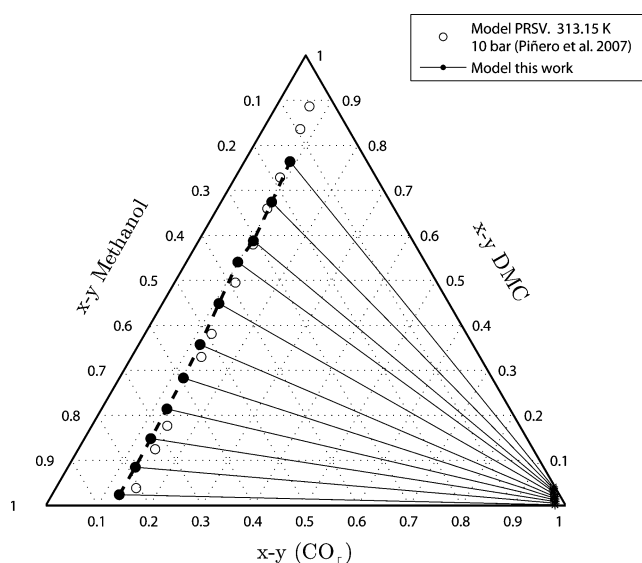

Figure 7. Predicted phase equilibrium diagram of the ternary system (CO$_2$–MeOH–DMC) at 313.15 K and 10 bar.[83] Dashed lines represent the VLE curve calculated with a $\gamma - \phi$ method; VLE tie lines are represented as solid lines.

agreement between predicted data with a $\phi - \phi$ method used by Piñero and co-workers and those calculated in this work with the $\gamma - \phi$ approach using the same EoS and mixing rule for the gas phase. Some discrepancies occur at high concentration of DMC in the liquid phase, perhaps due to the inaccuracy in the interaction parameters determined for the binary CO$_2$–DMC.

Results obtained in this part of the study show that the $\gamma - \phi$ approach—fugacity coefficients evaluated by the PRSV–1PVDW and activity coefficients with the UNIQUAC model—is able to correctly predict dew points of the different binary and ternary subsystems in the quaternary CO$_2$–MeOH–H$_2$O–DMC mixture at low and moderate pressures. The next part of this study is aimed at evaluating the dew point

for a reaction mixture of known chemical equilibrium composition, establishing the boundaries of a homogeneous gas phase reaction.

Chemical Equilibrium Modeling. *Equilibrium Constant.* Figure 8 shows the Gibb's free energy as a function of
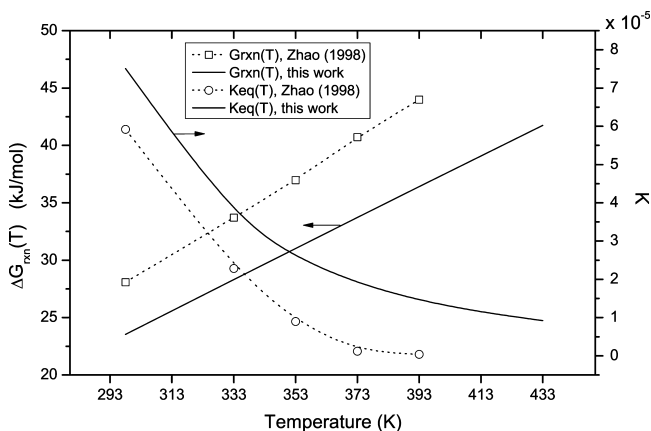

Figure 8. Temperature dependence of ΔG_{rxn}^{0} and K_{eq} in the direct synthesis of DMC.

temperature as well as the equilibrium constant, K_{eq}, for the direct synthesis of DMC. Results are compared with those reported by Zhao et al.[76]

According to Figure 8, ΔG_{rxn}^{0} increases with temperature and, consequently, the equilibrium constant K_{eq}, decreases. This trend is consistent with that reported by Cai et al.[17] and Zhao et al.[76] However, values in this work are expected to be more accurate because no assumptions were made regarding the $CO(O)(O)$ group contribution: the reported value by Khan et al.[80] was used. Nevertheless, experimental data for ΔG_f of DMC gas is still required to validate the results obtained.

Equilibrium Conversion. Since it is possible to estimate equilibrium conversions for a very large number of reaction conditions (P, T, Θ_{CO_2}, $y_{MeOH,0}$), a systematic analysis will be applied where the simplest conditions are evaluated first, and then the variables P, T, and feed molar ratio, Θ_{CO_2}, will be refined in order to set better values for achieving higher MeOH equilibrium conversions. Figure 9 shows the effect of
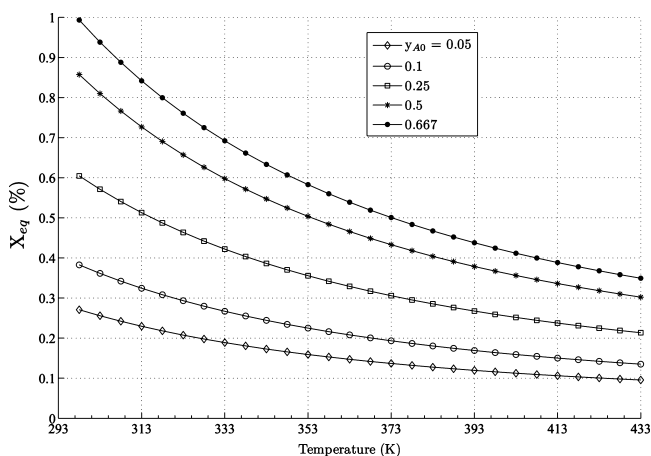

Figure 9. Effect of MeOH feed composition on its equilibrium conversion, X_{eq}. Θ_{CO_2} = 0.5, P = 1 atm.

temperature and MeOH feed concentration ($y_{MeOH,0}$) on the equilibrium conversion for the gas phase reaction when atmospheric pressure and stoichiometric CO_2/MeOH feed ratio are considered as constant values. It can be observed that the formation of products is favored as the initial MeOH concentration increases; however, a high feed MeOH concentration implies larger amounts of MeOH vapor under controlled flow, adding complexity to the system.

Figure 10 shows the effect of pressure and MeOH feed concentration ($y_{MeOH,0}$), considering a reactor temperature of
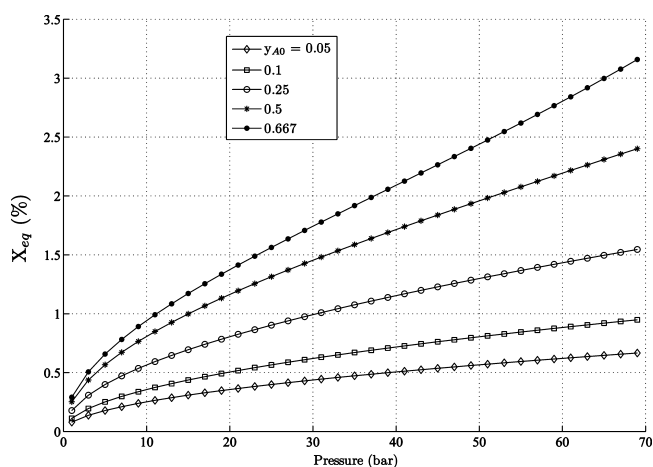

Figure 10. Effect of feed composition and reaction pressure on equilibrium conversion, X_{eq}. Θ_{CO_2} = 0.5, T = 473 K.

473 K. An increase in pressure favors MeOH conversion, reaching values above 2% at high feed MeOH concentrations. Although a temperature of 473 K was selected such that reactants and products coexist in the gas phase up to pressures near the critical region, this temperature adversely affects MeOH equilibrium conversion.

Previous reports[24,35,49,60] have shown that MeOH/CO_2 feed ratios influence DMC production. The effect of the reactant feed ratios and temperature on equilibrium conversion is shown in Figure 11. Intermediate conditions were used: 12 bar of pressure, which has already been experimentally reported,[64−66]
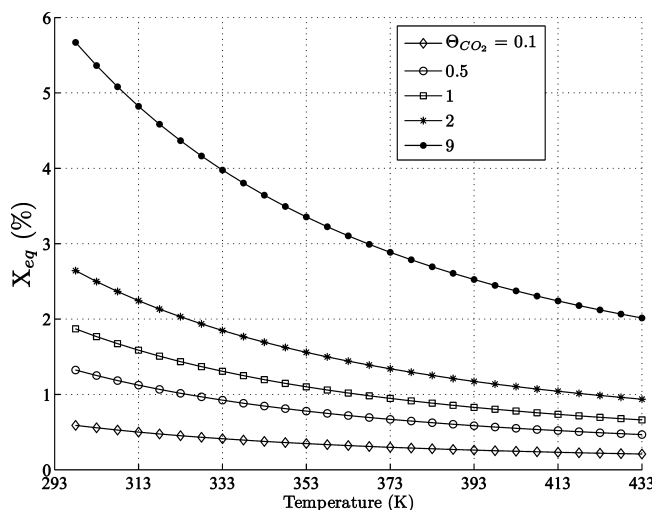

Figure 11. Effect of CO_2/MeOH feed ratios, Θ_{CO_2}, on equilibrium conversion, X_{eq}. P = 12 bar, $y_{MeOH,0}$ = 0.1.

and an initial MeOH fraction of 0.1 (from the analysis of Figure 9 and Figure 10). As can be observed in Figure 11, increasing CO_2/MeOH feed ratio favors MeOH equilibrium conversion. Moreover, a large excess of CO_2 (e.g., $\Theta_{CO_2} = 9$) may increase the equilibrium conversion significantly. The trend of equilibrium conversion with the temperature remains the same as shown in Figure 9.

Once favorable inlet conditions have been determined, the effect of pressure and temperature on equilibrium conversion were evaluated; results are shown in Figure 12. Equilibrium
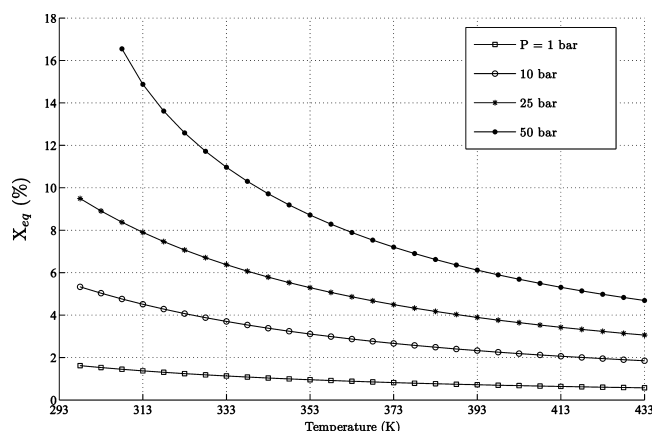

Figure 12. Effect of pressure and temperature on equilibrium conversion, X_{eq}. $\Theta_{CO_2} = 0.9$, $y_{MeOH,0} = 0.1$.

conversion is directly proportional to pressure and inversely proportional to temperature. However, such changes in temperature and pressure might cause condensation and thence the estimated conversions would be inaccurate if modeled at extreme conditions, i.e. high pressures and low temperatures.

It is important to note that although conversions remain low, such as conventional reactions limited by chemical equilibrium, certain enhancement in conversion can be expected through new approaches, for example, using membrane catalytic reactors, in order to make the direct synthesis of DMC a more "feasible" route.

X_{eq} and Dew Point for Quaternary Mixture. In order to establish the limits of temperature and pressure to prevent partial condensation of the reaction mixture, dew curves for several mixture compositions under chemical equilibrium were calculated, Figure 13. A hypothetical perfectly mixed continuous reactor, where the DMC reaction occurs very rapidly was considered. The conditions of P, T, and feed composition used to generate those profiles, as well as the calculated equilibrium conversion are presented in Table 6. All conversions are calculated with respect to MeOH; pressure was varied between 1 and 25 bar while the temperature was fixed at 298 K, representing the most favorable case for the reaction.

Figure 13 shows the zones of coexistence of monophasic (vapor) and biphasic (liquid + vapor) state for five equilibrium conditions summarized in Table 6. The equilibrium conversions for the initial mixture composition (when no condensation is assumed) are compared with those under noncondensation conditions.

Several remarks can be made from Figure 13 and Table 6. From a practical standpoint, feed conditions of mixture 1, Figure 13a, could be the simplest conditions for carrying out

the reaction. Here, methanol conversion is 1.61%, but the pressure of the system can still be increased without reaching the dew curve. Thus, by an isothermal increase of pressure, the dew curve can be intercepted obtaining a more favorable reaction pressure without increasing the reaction temperature. In this way, a conversion of 2.085% (see last column in Table 6) could be achieved near atmospheric pressure (1.66 bar) and room temperature. Although this conversion is low compared with other initial conditions, gas-phase production of DMC could be attractive under these mild pressure conditions. At a pressure of 12 bar and room temperature, a remarkable increase in the initial equilibrium conversion can be observed in Figure 13 panels b, c, and d, reaching values of 4.16, 4.8, and 5.91%, respectively. However, at those P and T, partial condensation of the reaction mixture will occur (i.e., equilibrium conversions are located inside L−V biphasic region). Therefore, at P = 12 bar, the temperature must be increased to reach the vapor zone (i.e., gas-phase reaction), leading to lower equilibrium conversion. The new conversion values calculated (marked with an asterisk (∗)) are 1.5, 1.99, and 3.8% for the three feed ratios and compositions shown in Table 6, respectively. It is clear that neither reaction mixture 2 nor 3 (stoichiometric and equimolar feed compositions between MeOH and CO_2, respectively) are better than mixture 1 since gas-phase equilibrium conversions at noncondensation conditions are smaller. Moreover, pressure has been increased from 1.66 to 12 bar and the reaction temperature is higher. Consequently, the improvement in conversion does not offset the increase in operational costs. On the other hand, under the noncondensing conditions of mixture 4 an equilibrium conversion of 3.8% is attained, which would be more attractive to obtain DMC.

Similarly, the effect of pressure, feed ratio, and temperature for mixture 5, indicate that initial excess of CO_2 favors higher conversion. Although in an actual system the pressure could be increased to larger values, this variable was kept below 25 bar in order to obtain values within the scope of the proposed thermodynamic model. Under the initial conditions of mixture 5, the equilibrium conversion (X_{eq0}) is significantly improved to 9.49%, five times larger than conversions achieved at atmospheric pressure; however, this conversion falls to about 5% when the system is evaluated under noncondensing conditions. The conversion increase is still considerable, and the reaction temperature increase needed (from 298 to 358 K) is not quite significant.

If pressure increases, the temperature of the system must also be increased such that the reaction mixture will not fall in the L−V region. Moreover, the larger the amount of MeOH in the feed mixture, the higher the temperature required for conducting the gas-phase reaction; thence it is advisable to carry out the reaction under an excess of CO_2. Camy et al.[82] have also investigated the number of phases existing in the reactor as a function of pressure and temperature and remarked that the vapor phase zone is restricted to high temperature and low pressure. Furthermore, the "available" vapor region increases by increasing CO_2 in the reacting mixture. For a mixture containing a high concentration of MeOH or DMC, the vapor zone is very narrow and is only present at low pressure and high temperature. It is important to note that the present results are theoretical. Experimental data on VLE of the quaternary mixture will allow the extrapolation of the results to higher pressures and temperatures.

Equilibrium Dew Pressure. With the aim of evaluating the boundaries of the gas phase, Figure 14 shows the dew pressure
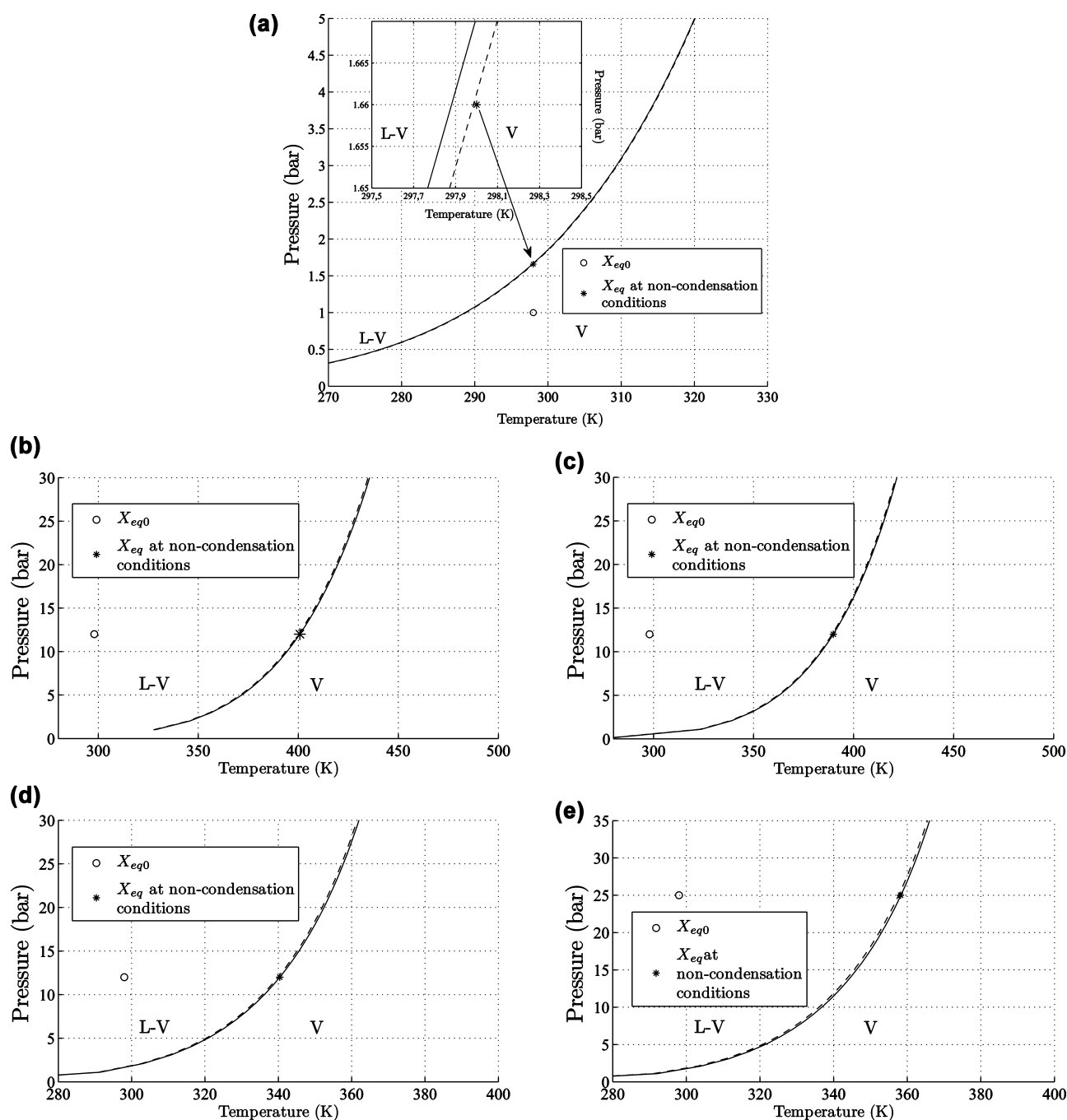
Figure 13. $p-T$ diagrams for five different quaternary reacting mixtures. Dew curves for initial reacting mixture (solid line) and for noncondensation compositions (dashed line). Symbols (O, *) represent the calculated equilibrium conversions under conditions shown in Table 6. The letter "L−V" refers to a biphasic state and the vapor region is marked with the letter "V".

Table 6. Reacting Mixture Composition in Chemical Equilibrium

			feed composition			reacting mixture composition at equilibrium				noncondensation conditions		
mixture	P (bar)	T (K)	y_{MeOH}	y_{CO_2}	X_{eq} %	y_{MeOH}	y_{CO_2}	y_{DMC}	y_{H2O}	P (bar)	T (K)	X_{eq} (%)
1	1	298	0.1	0.9	1.6171	0.0985	0.8999	8.0919×10^{-4}	8.0919×10^{-4}	1.66	298	2.085
2	12	298	0.667	0.333	4.1613	0.6479	0.3240	0.0141	0.0141	12	400.8	1.525
3	12	298	0.5	0.5	4.8065	0.4818	0.4939	0.0122	0.0122	12	389.9	1.99
4	12	298	0.1	0.9	5.9165	0.0943	0.8997	0.003	0.003	12	340.4	3.828
5	25	298	0.1	0.9	9.4921	0.0909	0.8995	0.0048	0.0048	25	358.2	5.061

at different temperature and inlet $MeOH/CO_2$ ratios for the quaternary mixture at chemical equilibrium.
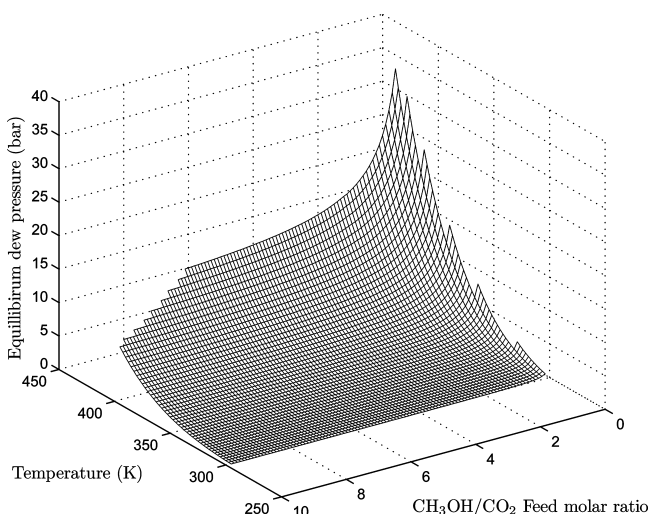

Figure 14. Effect of CH_3OH/CO_2 feed ratio and reaction temperature on equilibrium dew pressure for quaternary mixture.

Any point located above the surface in Figure 14 will undergo partial condensation. Therefore, the reaction pressure for a given temperature and inlet $MeOH/CO_2$ ratio is limited by the equilibrium dew pressure of the quaternary mixture, which is indicated by the surface. It can be noted that as higher MeOH concentrations are fed, equilibrium dew pressures are lower, leading to lower equilibrium conversions, as discussed previously. Otherwise, if the MeOH concentration in the feed is decreased, a higher dew pressure is observed; however, a higher temperature is required, which would lead to a smaller reaction extent. In this way, Figure 14 is a very useful tool to determine the most convenient conditions for the gas-phase synthesis of DMC from MeOH and CO_2. 2D views of Figure 14 are included as Supporting Information in order to facilitate the use of the 3D plot; the figures show P versus T curves for various CH_3OH/CO_2 feed ratios.

CONCLUSIONS

Benson's group contribution method used to estimate ΔH_f, ΔG_f, and C_p for DMC showed to be a reliable approach when compared with available thermodynamic data. The direct synthesis of DMC in the gas phase is a nonspontaneous and exothermic reaction and from chemical equilibrium modeling it can be concluded that increasing pressure favors equilibrium conversion. Otherwise, increasing temperature has a negative effect on equilibrium conversion.

Using reported binary interaction parameters and a $\gamma - \phi$ model, dew curves of binary subsystems for the quaternary mixture (i.e., for the CO_2-H_2O, CO_2-MeOH, CO_2-DMC, $DMC-MeOH$, $DMC-H_2O$, $MeOH-H_2O$ systems) were predicted in good agreement with experimental data at mild pressure–temperature conditions, except for CO_2-DMC system where results were slightly less accurate.

The ability of the model to predict dew curves for the quaternary mixture at different equilibrium conditions was evaluated. From simultaneous analysis of chemical equilibrium and phase behavior it is concluded that a large excess of CO_2 improves not only DMC yield but also allows running the reaction in a homogeneous gas phase without significant temperature increase, which is undesirable if a large reaction extent is desired.

ASSOCIATED CONTENT

ⓢ Supporting Information

Results of average absolute deviations (AAD%) of pressure and vapor phase composition for six binary subsystems; 2D views of Figure 14 in order to facilitate its use: the figures show P vs T curves for various CH_3OH/CO_2 feed ratios. This material is available free of charge via the Internet at http://pubs.acs.org.

AUTHOR INFORMATION

Corresponding Author

*E-mail: fbustama@udea.edu.co. Tel.: +57 (4) 2198535. Fax: +57 (4) 2196565.

Notes

The authors declare no competing financial interest.

ACKNOWLEDGMENTS

NOMENCLATURE

a activity coefficient
A_{ij} binary interaction parameter in UNIQUAC model [cal mol^{-1}]
C_P heat capacity [J mol^{-1} K^{-1}]
G Gibbs Free Energy [kJ mol^{-1}]
H enthalpy [kJ mol^{-1}]
k_{ij}, l_{ij} binary interaction parameter in 1PVDW mixing rule
K equilibrium constant
L liquid
n number of experimental points
N_e number of elements
N_k number of groups
P pressure [Pa or bar]
P^0 standard Pressure, 1 bar
R universal gas constant, 8.314 [J mol^{-1} K^{-1}]
S entropy [J mol^{-1} K^{-1}]
S_s symmetry entropy [J mol^{-1} K^{-1}]
S_e entropy of element e [J mol^{-1} K^{-1}]
T temperature (K)
V vapor
x liquid molar fraction
y vapor molar fraction

Greek Letters

Δ change
Θ CO_2/CH_3OH feed molar ratio
ϕ_i^0 fugacity coefficient of pure specie i
$\hat{\phi}_i$ fugacity coefficient of specie i in the mixture

Subscripts

0   initial
e   element
eq   at equilibrium
f   formation
i,j   component
k   group number in Benson's method
rxn   reaction

Superscripts

0   standard state
cal   calculated
exp   experimental

■ REFERENCES

(1) Ono, Y. Dimethyl carbonate for environmentally benign reactions. *Catal. Today* **1997**, *35*, 15−25.

(2) Pacheco, M. A.; Marshall, C. L. Review of dimethyl carbonate (DMC) Manufacture and its characteristics as a fuel additive. *Energy Fuel* **1997**, *11*, 2−29.

(3) Delledonne, D.; Rivetti, F.; Romano, U. Developments in the production and application of dimethylcarbonate. *Appl. Catal., A* **2001**, *221*, 241−251.

(4) Sakakura, T.; Choi, J.-C.; Yasuda, H. Transformation of carbon dioxide. *Chem. Rev.* **2007**, *107*, 2365−2387.

(5) Ma, J.; Sun, N.; Zhang, X.; Zhao, N.; Xiao, F.; Wei, W.; Sun, Y. A short review of catalysis for CO_2 conversion. *Catal. Today* **2009**, *148*, 221−231.

(6) Leino, E.; Mäki-Arvela, P.; Eta, V.; Murzin, D. Y.; Salmi, T.; Mikkola, J. P. Conventional synthesis methods of short-chain dialkylcarbonates and novel production technology via direct route from alcohol and waste CO_2. *Appl. Catal., A* **2010**, *221*, 241−251.

(7) Keller, N.; Rebmann, G.; Keller, V. Review: Catalysts, mechanisms and industrial processes for the dimethylcarbonate synthesis. *J. Mol. Catal. A: Chem.* **2010**, *317*, 1−18.

(8) Choi, J.-C.; Sakakura, T.; Sako, T. Reaction of dialkyltin methoxide with carbon dioxide relevant to the mechanism of catalytic carbonate synthesis. *J. Am. Chem. Soc.* **1999**, *121*, 3793−3794.

(9) Ballivet-Tkatchenko, D.; Douteau, O.; Stutzmann, S. Reactivity of carbon dioxide with *n*-butyl(phenoxy)-, (alkoxy)-, and (oxo)stannanes: Insight into dimethyl carbonate synthesis. *Organometallics* **2000**, *19*, 4563−4567.

(10) Ballivet-Tkatchenko, D.; Jerphagnon, T.; Ligabue, R.; Plasseraud, L.; Poinsot, D. The role of distannoxanes in the synthesis of dimethyl carbonate from carbon dioxide. *Appl. Catal., A* **2003**, *255*, 93−99.

(11) Ballivet-Tkatchenko, D.; Ligabue, R. A.; Plasseraud, L. Synthesis of dimethyl carbonate in supercritical carbon dioxide. *Braz. J. Chem. Eng* **2006**, *23*, 111−116.

(12) Ballivet-Tkatchenko, D.; Chambrey, S.; Keiski, R.; Ligabue, R.; Plasseraud, L.; Richard, P.; Turunen, H. Direct synthesis of dimethyl carbonate with supercritical carbon dioxide: Characterization of a key organotin oxide intermediate. *Catal. Today* **2006**, *115*, 80−87.

(13) Plasseraud, L.; Ballivet-Tkatchenko, D.; Cattey, H.; Chambrey, S.; Ligabue, R.; Richard, P.; Willem, R.; Biesemans, M. Di-*n*-butyltin oxide as a chemical carbon dioxide capturer. *J. Organomet. Chem.* **2010**, *695*, 1618−1626.

(14) Fan, B.; Zhang, J.; Li, R.; Fan, W. In situ preparation of functional heterogeneous organotin catalyst tethered on SBA-15. *Catal. Lett.* **2008**, *121*, 297−302.

(15) Fan, B.; Li, H.; Fan, W.; Zhang, J.; Li, R. Organotin compounds immobilized on mesoporous silicas as heterogeneous catalysts for direct synthesis of dimethyl carbonate from methanol and carbon dioxide. *Appl. Catal., A* **2010**, *372*, 94−102.

(16) Fan, B.; Li, H.; Fan, W.; Qin, Z.; Li, R. Direct synthesis of dimethyl carbonate from methanol and carbon dioxide over organotin-functionalized mesoporous benzene-silica. *Pure Appl. Chem.* **2012**, *84*, 663−673.

(17) Cai, Q.; Lu, B.; Guo, L.; Shan, Y. Studies on synthesis of dimethyl carbonate from methanol and carbon dioxide. *Catal. Commun.* **2009**, *10*, 605−609.

(18) Sakakura, T.; Saito, Y.; Okano, M.; Choi, J.-C.; Sako, T. Selective conversion of carbon dioxide to dimethyl carbonate by molecular catalysis. *J. Org. Chem.* **1998**, *63*, 7095−7096.

(19) Isaacs, N. S.; O'sullivan, B.; Verhaelen, C. High pressure routes to dimethyl carbonate from supercritical carbon dioxide. *Tetrahedron* **1999**, *55*, 11949−11956.

(20) Sakakura, T.; Choi, J.-C.; Saito, Y.; Masuda, T.; Sako, T.; Oriyama, T. Metal-catalyzed dimethyl carbonate synthesis from carbon dioxide and acetals. *J. Org. Chem.* **1999**, *64*, 4506−4508.

(21) Sakakura, T.; Choi, J.-C.; Saito, Y.; Sako, T. Synthesis of dimethyl carbonate from carbon dioxide: catalysis and mechanism. *Polyhedron* **2000**, *19*, 573−576.

(22) Choi, J.-C.; He, L.-N.; Yasuda, H.; Sakakura, T. Selective and high yield synthesis of dimethyl carbonate directly from carbon dioxide and methanol. *Green Chem.* **2002**, *4*, 230−234.

(23) Zhao, T.; Han, Y.; Sun, Y. Supercritical synthesis of dimethyl carbonate from CO_2 and methanol. *Stud. Surf. Sci. Catal.* **2000**, *130*, 461−466.

(24) Zhao, T.; Han, Y.; Sun, Y. Novel reaction route for dimethyl carbonate synthesis from CO_2 and methanol. *Fuel Process. Technol.* **2000**, *62*, 187−194.

(25) Sun, Y. Chemicals from CO_2 via heterogeneous catalysis at moderate conditions. *Stud. Surf. Sci. Catal.* **2004**, *153*, 9−16.

(26) Aresta, M.; Dibenedetto, A.; Fracchiolla, E.; Giannoccaro, P.; Pastore, C.; Pápai, I.; Schubert, G. Mechanism of formation of organic carbonates from aliphatic alcohols and carbon dioxide under mild conditions promoted by carbodiimides. DFT calculation and experimental study. *J. Org. Chem.* **2005**, *70*, 6177−6186.

(27) Dibenedetto, A.; Pastore, C.; Aresta, M. Direct carboxylation of alcohols to organic carbonates: Comparison of the group 5 element alkoxides catalytic activity: An insight into the reaction mechanism and its key steps. *Catal. Today* **2006**, *115*, 88−94.

(28) Aresta, M.; Dibenedetto, A.; Pastore, C.; Pápai, I.; Schubert, G. Reaction mechanism of the direct carboxylation of methanol to dimethylcarbonate: Experimental and theoretical studies. *Top. Catal.* **2006**, *40*, 71−81.

(29) Aresta, M.; Dibenedetto, A.; Nocito, F.; Pastore, C. Comparison of the behaviour of supported homogeneous catalysts in the synthesis of dimethylcarbonate from methanol and carbon dioxide: Polystyrene-grafted tin−metallorganic species versus silesquioxanes linked Nb-methoxo species. *Inorg. Chim. Acta* **2008**, *361*, 3215−3220.

(30) Aresta, M.; Dibenedetto, A.; Nocito, F.; Angelini, A.; Gabriele, B.; Negri, S. D. Synthesis and characterization of a novel polystyrene-tethered niobium methoxo species. Its application in the CO_2-based carboxylation of methanol to afford dimethyl carbonate. *Appl. Catal., A* **2010**, *387*, 113−118.

(31) Fang, S.; Fujimoto, K. Direct synthesis of dimethyl carbonate from carbon dioxide and methanol catalyzed by base. *Appl. Catal., A* **1996**, *142*, L1−L3.

(32) Fujita, S.; Bhanage, B. M.; Ikushima, Y.; Arai, M. Synthesis of dimethyl carbonate from carbon dioxide and methanol in the presence of methyl iodide and base catalysts under mild conditions: Effect of reaction conditions and reaction mechanism. *Green Chem.* **2001**, *3*, 87−91.

(33) Cai, Q. H.; Jin, C.; Lu, B.; Tangbo, H.; Shana, Y. Synthesis of dimethyl carbonate from methanol and carbon dioxide using potassium methoxide as catalyst under mild conditions. *Catal. Lett.* **2005**, *103*, 225−228.

(34) Wang, H.; Lu, B.; Cai, Q. H.; Wu, F.; Shan, Y. K. Synthesis of dimethyl carbonate from methanol and carbon dioxide catalyzed by potassium hydroxide under mild conditions. *Chin. Chem. Lett.* **2005**, *16*, 1267−1270.

(35) Tomishige, K.; Ikeda, Y.; Sakaihori, T.; Fujimoto, K. A novel method of direct synthesis of dimethyl carbonate from methanol and carbon dioxide catalyzed by zirconia. *Catal. Lett.* **1999**, *58*, 225−229.

(36) Tomishige, K.; Ikeda, Y.; Sakaihori, T.; Fujimoto, K. Catalytic properties and structure of zirconia catalysts for direct synthesis of dimethyl carbonate from methanol and carbon dioxide. *J. Catal.* **2000**, *192*, 355−362.

(37) Tomishige, K.; Furusawa, Y.; Ikeda, Y.; Asadullah, M.; Fujimoto, K. $CeO_2−ZrO_2$ solid solution catalyst for selective synthesis of dimethyl carbonate from methanol and carbon dioxide. *Catal. Lett.* **2001**, *76*, 71−74.

(38) Tomishige, K.; Kunimori, K. Catalytic and direct synthesis of dimethyl carbonate starting from carbon dioxide using $CeO_2−ZrO_2$

solid solution heterogeneous catalyst: Effect of H_2O removal from the reaction system. *Appl. Catal., A* **2002**, *237*, 103−109.

(39) Han, G. B.; Park, N. K.; Jun, J. H.; Chang, W. C.; Lee, B. G.; Ahn, B. S.; Ryu, S. O.; Lee, T. J. Chemicals from CO_2 via heterogeneous catalysis at moderate conditions. *Stud. Surf. Sci. Catal.* **2004**, *153*, 181−184.

(40) Zhang, Z.-F.; Liu, Z.-T.; Liu, Z.-W.; Lu, J. DMC formation over $Ce_{0.5}Zr_{0.5}O_2$ prepared by complex-decomposition method. *Catal. Lett.* **2009**, *129*, 428−436.

(41) Zhang, Z.-F.; Liu, Z.-W.; Lu, J.; Liu, Z.-T. Synthesis of dimethyl carbonate from carbon dioxide and methanol over $Ce_xZr_{1−x}O_2$ and $[EMIM]Br/Ce_{0.5}Zr_{0.5}O_2$. *Ind. Eng. Chem. Res.* **2011**, *50*, 1981−1988.

(42) Jiang, C.; Guo, Y.; Wang, C.; Hu, C.; Wu, Y.; Wang, E. Synthesis of dimethyl carbonate from methanol and carbon dioxide in the presence of polyoxometalates under mild conditions. *Appl. Catal., A* **2003**, *256*, 203−212.

(43) Ikeda, Y.; Sakaihori, T.; Tomishige, K.; Fujimoto, K. Promoting effect of phosphoric acid on zirconia catalysts in selective synthesis of dimethyl carbonate from methanol and carbon dioxide. *Catal. Lett.* **2000**, *66*, 59−62.

(44) Ikeda, Y.; Asadullah, M.; Fujimoto, K.; Tomishige, K. Structure of the active sites on H_3PO_4/ZrO_2 catalysts for dimethyl carbonate synthesis from methanol and carbon dioxide. *J. Phys. Chem. B* **2001**, *105*, 10653−10658.

(45) Eta, V.; Mäki-Arvela, P.; Leino, A.-R.; Kordás, K.; Salmi, T.; Murzin, D. Y.; Mikkola, J.-P. Synthesis of dimethyl carbonate from methanol and carbon dioxide: Circumventing thermodynamic limitations. *Ind. Eng. Chem. Res.* **2010**, *49*, 9609−9617.

(46) La, K. W.; Song, I. K. Direct synthesis of dimethyl carbonate from CH_3OH and CO_2 by $H_3PW_{12}O_{40}/Ce_xTi_{1−x}O_2$ catalyst. *React. Kinet. Catal. Lett.* **2006**, *89*, 303−309.

(47) La, K. W.; Jung, J. C.; Kim, H.; Baeck, S.-H.; Song, I. K. Effect of acid−base properties of $H_3PW_{12}O_{40}/Ce_xTi_{1−x}O_2$ catalysts on the direct synthesis of dimethyl carbonate from methanol and carbon dioxide: A TPD study of $H_3PW_{12}O_{40}/Ce_xTi_{1−x}O_2$ catalysts. *J. Mol. Catal. A: Chem.* **2007**, *269*, 41−45.

(48) Lee, H. J.; Park, S.; Jung, J. C.; Song, I. K. Direct synthesis of dimethyl carbonate from methanol and carbon dioxide over $H_3PW_{12}O_{40}/Ce_xZr_{1−x}O_2$ catalysts: Effect of acidity of the catalysts. *Korean J. Chem. Eng.* **2011**, *28*, 1518−1522.

(49) Yoshid, Y.; Arai, Y.; Kado, S.; Kunimori, K.; Tomishige, K. Direct synthesis of organic carbonates from the reaction of CO_2 with methanol and ethanol over CeO_2 catalysts. *Catal. Today* **2006**, *115*, 95−101.

(50) Aresta, M.; Dibenedetto, A.; Pastore, C.; Angelini, A.; Aresta, B.; Pápai, I. Influence of Al_2O_3 on the performance of CeO_2 used as catalyst in the direct carboxylation of methanol to dimethylcarbonate and the elucidation of the reaction mechanism. *J. Catal.* **2010**, *269*, 44−52.

(51) Lee, H. J.; Park, S.; Song, I. K.; Jung, J. C. Direct Synthesis of Dimethyl Carbonate from Methanol and Carbon Dioxide over $Ga_2O_3/Ce_{0.6}Zr_{0.4}O_2$ Catalysts: Effect of Acidity and Basicity of the Catalysts. *Catal. Lett.* **2011**, *141*, 531−537.

(52) Lee, H. J.; Joe, W.; Song, I. K. Direct synthesis of dimethyl carbonate from methanol and carbon dioxide over transition metal oxide/$Ce_{0.6}Zr_{0.4}O_2$ catalysts: Effect of acidity and basicity of the catalysts. *Korean J. Chem. Eng.* **2012**, *29*, 317−322.

(53) Eta, V.; Mäki-Arvela, P.; Salminen, E.; Salmi, T.; Murzin, D. Y.; Mikkola, J.-P. The Effect of alkoxide ionic liquids on the synthesis of dimethyl carbonate from CO_2 and methanol over ZrO_2−MgO. *Catal. Lett.* **2011**, *141*, 1254−1261.

(54) Ballivet-Tkatchenko, D.; dos Santos, J. H.; Philippot, K.; Vasireddy, S. Carbon dioxide conversion to dimethyl carbonate: The effect of silica as support for SnO_2 and ZrO_2 catalysts. *C. R. Chim.* **2011**, *14*, 780−785.

(55) Allaoui, L.; Aouissi, A. Effect of the Bronsted acidity on the behavior of CO_2 methanol reaction. *J. Mol. Catal. A: Chem.* **2006**, *259*, 281−285.

(56) Honda, M.; Suzuki, A.; Noorjahan, B.; Fujimoto, K.; Suzuki, K.; Tomishige, K. Low pressure CO_2 to dimethyl carbonate by the reaction with methanol promoted by acetonitrile hydration. *Chem. Commun.* **2009**, 4596−4598.

(57) Aouissi, A.; Apblett, A. W.; AL-Othman, Z. A.; Al-Amro, A. Direct synthesis of dimethyl carbonate from methanol and carbon dioxide using heteropolyoxometalates: The effects of cation and addenda atoms. *Transition Met. Chem. (Dordrecht, The Netherlands)* **2010**, *35*, 927−931.

(58) Aouissi, A.; Al-Deyab, S. S.; Al-Owais, A.; Al-Amro, A. Reactivity of heteropolytungstate and heteropolymolybdate metal transition salts in the synthesis of dimethyl carbonate from methanol and CO_2. *J. Mol. Catal. A: Chem.* **2010**, *11*, 2770−2779.

(59) Zhong, S.; Wang, J.; Xiao, X.; Li, H. Dimethyl carbonate synthesis from carbon dioxide and methanol over Ni−Cu/MoSiO-(VSiO) catalysts. *Stud. Surf. Sci. Catal.* **2000**, *130*, 1565−1570.

(60) Li, C. F.; Zhong, S. H. Study on application of membrane reactor in direct synthesis DMC from CO_2 and CH_3OH over Cu−KF/MgSiO catalyst. *Catal. Today* **2003**, *82*, 83−90.

(61) Wu, X.; Xiao, M.; Meng, Y.; Lu, Y. Direct synthesis of dimethyl carbonate on H_3PO_4 modified V_2O_5. *J. Mol. Catal. A: Chem.* **2005**, *238*, 158−162.

(62) Wu, X.; Meng, Y.; Xiao, M.; Lu, Y. Direct synthesis of dimethyl carbonate (DMC) using Cu-Ni/VSO as catalyst. *J. Mol. Catal. A: Chem.* **2006**, *249*, 93−97.

(63) Wang, X.; Xiao, M.; Wang, S.; Lu, Y.; Meng, Y. Direct synthesis of dimethyl carbonate from carbon dioxide and methanol using supported copper (Ni, V, O) catalyst with photo-assistance. *J. Mol. Catal. A: Chem.* **2007**, *278*, 92−96.

(64) Bian, J.; Xiao, M.; Wang, S. J.; Lu, Y. X.; Meng, Y. Z. Highly effective direct synthesis of DMC from CH_3OH and CO_2 using novel Cu-Ni/C bimetallic composite catalysts. *Chin. Chem. Lett.* **2009**, *20*, 352−355.

(65) Bian, J.; Xiao, M.; Wang, S.; Wang, X.; Lu, Y.; Meng, Y. Highly effective synthesis of dimethyl carbonate from methanol and carbon dioxide using a novel copper−nickel/graphite bimetallic nano-composite catalyst. *Chem. Eng. J. (Amsterdam, The Netherlands)* **2009**, *147*, 287−296.

(66) Bian, J.; Xiao, M.; Wang, S.-J.; Lu, Y.-X.; Meng, Y.-Z. Carbon nanotubes supported Cu−Ni bimetallic catalysts and their properties for the direct synthesis of dimethyl carbonate from methanol and carbon dioxide. *Appl. Surf. Sci.* **2009**, *255*, 7188−7196.

(67) Bian, J.; Xiao, M.; Wang, S.; Lu, Y.; Meng, Y. Direct synthesis of DMC from CH_3OH and CO_2 over V−doped Cu−Ni/AC catalysts. *Catal. Commun.* **2009**, *10*, 1142−1145.

(68) Bian, J.; Xiao, M.; Wang, S.; Lu, Y.; Meng, Y. Novel application of thermally expanded graphite as the support of catalysts for direct synthesis of DMC from CH_3OH and CO_2. *J. Colloid Interface Sci.* **2009**, *334*, 50−57.

(69) Bian, J.; Xiao, M.; Wang, S.; Lu, Y.; Meng, Y. Graphite oxide as a novel host material of catalytically active Cu−Ni bimetallic nano-particles. *Catal. Commun.* **2009**, *10*, 1529−1533.

(70) Bian, J.; Wei, X. W.; Wang, L.; Guan, Z. P. Graphene nanosheet as support of catalytically active metal particles in DMC synthesis. *Chin. Chem. Lett.* **2011**, *22*, 57−60.

(71) Almusaiteer, K. Synthesis of dimethyl carbonate (DMC) from methanol and CO_2 over Rh-supported catalyst. *Catal. Commun.* **2009**, *10*, 1127−1131.

(72) Bian, J.; Wei, X.; Jin, Y.; Wang, L.; Luan, D.; Guan, Z. Direct synthesis of dimethyl carbonate over activated carbon supported Cu−based catalysts. *Chem. Eng. J.* **2010**, *165*, 686−692.

(73) Aouissi, A.; Al-Othman, Z. A.; Al-Amro, A. Gas-phase synthesis of dimethyl carbonate from methanol and carbon dioxide over $Co_{1.5}PW_{12}O_{40}$ Keggin-type heteropolyanion. *Int. J. Mol. Sci.* **2010**, *11*, 1343−1351.

(74) Chen, Y.; Xiao, M.; Wang, S.; Han, D.; Lu, Y.; Meng, Y. Porous diatomite−immobilized Cu−Ni bimetallic nanocatalysts for direct synthesis of dimethyl carbonate. *J. Nanomater.* **2012**, *2012*, 1−8.

(75) Sakakura, T.; Kohno, K. The synthesis of organic carbonates from carbon dioxide. *Chem. Commun.* **2009**, 1312−1330.

(76) Zhao, T.; Han, Y.; Sun, Y. Thermodynamic estimation of direct synthesis of dimethyl carbonate from CH_3OH and CO_2. *Nat. Gas. Chem. Ind. (Chin.)* **1998**, *23*, 52−56.

(77) Lide, D. R., Ed. *Handbook of Chemistry and Physics*, 90th ed.; CRC Press, Taylor and Francis: Boca Raton, FL, 2010.

(78) Poling, B. E., Prausnitz, J. M., O'Connell, J. P., Eds. *The Properties of Gases and Liquids*, 5th ed.; McGraw-Hill: New York, 2001.

(79) Steele, W. V.; Chirico, R. D.; Knipmeyer, S. E.; Nguyen, A.; Smith, N. K. Thermodynamic properties and ideal-gas enthalpies of formation for dicyclohexyl sulfide, diethylenetriamine, di-*n*-octyl sulfide, dimethyl carbonate, piperazine, hexachloroprop-1-ene, tetrakis-(dimethylamino)ethylene, *N,N'*-bis-(2-hydroxyethyl)ethylenediamine, and 1,2,4-triazolo[1,5-*a*] pyrimidine. *J. Chem. Eng. Data* **1997**, *42*, 1037−1052.

(80) Khan, S. S.; Yu, X.; Wade, J. R.; Malmgren, R. D.; Broadbelt, L. J. Thermochemistry of radicals and molecules relevant to atmospheric chemistry: determination of group additivity values using G3//B3LYP Theory. *J. Phys. Chem. A* **2009**, *113*, 5176−5194.

(81) Hougen, O., Watson, K., Ragatz, R. A., Eds. *Chemical Process Principles. Part 1*; John Wiley & Sons: New York, 1954.

(82) Camy, S.; Pic, J. S.; Badens, E.; Condoret, J. S. Fluid phase equilibria of the reacting mixture in the dimethyl carbonate synthesis from supercritical CO_2. *J. Supercrit. Fluids* **2003**, *25*, 19−32.

(83) Piñero, R.; García, J.; Sokolova, M.; Cocero, M. J. Modelling of the phase behavior for the direct synthesis of dimethyl carbonate from CO_2 and methanol at supercritical or near critical conditions. *J. Chem. Thermodyn.* **2007**, *39*, 536−549.

(84) Redlich, O.; Kwong, J. N. S. On the thermodynamics of solution. V: An equation of state. Fugacities of gaseous solutions. *Chem. Rev.* **1949**, *44*, 233−244.

(85) Huron, J.; Vidal, J. New mixing rules in simple equations of state for representing vapor−liquid equilibria of strongly non-ideal mixtures. *Fluid Phase Equilib.* **1979**, *3*, 255−271.

(86) Dahl, S.; Michelsen, M. L. High-pressure vapor−liquid equilibrium with a UNIFAC-based equation of state. *AIChE J.* **1990**, *36*, 1829−1836.

(87) Stryjek, R.; Vera, J. H. PRSV: An improved Peng−Robinson equation of state for pure compounds and mixtures. *Can. J. Chem. Eng.* **1986**, *64*, 323−333.

(88) Orbey, H., Sandler, S. I., Eds. *Modelling vapor−liquid equilibria: Cubic equation of state and their mixing rules*, 25th ed.; Cambridge University Press: Cambridge, UK, 1998.

(89) Abrams, D. S.; Prausnitz, J. M. Statistical thermodynamics of liquid mixture: A new expression for the excess Gibbs energy of partly or complete miscible systems. *AIChE J.* **1975**, *21*, 116−128.

(90) Anderson, T. F.; Prausnitz, J. M. Application of the UNIQUAC equation to calculation of multi-component phase equilibria. 1. Vapor−liquid equilibria. *Ind. Eng. Chem. Process Des. Dev.* **1978**, *17*, 552−560.

(91) Ma, X. B.; Liu, X. G.; Li, Z. H.; Xu, G. H. Vapor−liquid equilibria for the ternary system methanol + dimethyl carbonate + dimethyl oxalate and constituent binary systems at different temperatures. *Fluid Phase Equilib.* **2004**, *221*, 51−56.

(92) de la Torre, J.; Chafer, A.; Berna, A.; Muñoz, R. Liquid−liquid equilibria of the system dimethyl carbonate + methanol + water at different temperatures. *Fluid Phase Equilib.* **2006**, *247*, 40−46.

(93) Chiehming, J. C.; Kou-Lung, C.; Chang-Yih, D. A new apparatus for the determination of $P−x−y$ diagrams and Henry's constants in high pressure alcohols with critical carbon dioxide. *J. Supercrit. Fluids* **1998**, *12*, 223−237.

(94) Secuianu, C.; Feroiu, V.; Geană, D. Phase equilibria experiments and calculations for carbon dioxide + methanol binary system. *Cent. Eur. J. Chem.* **2009**, *7*, 1−7.

(95) Kwak, C.; Sandler, S. I.; Byun, H. S. Correlation of vapor−liquid equilibria for binary mixtures with free energy-based equation of state mixing rules: Carbon dioxide with alcohols, hydrocarbons, and several other compounds. *Korean J. Chem. Eng.* **2006**, *23*, 1016−1022.

(96) Lee, M. H.; Yim, J.-H.; Kang, J. W.; Lim, J. S. Measurement of VLE data of carbon dioxide + dimethyl carbonate system for the direct synthesis of dimethyl carbonate using supercritical CO_2 and methanol. *Fluid Phase Equilib.* **2012**, *318*, 77−82.

(97) Pappa, G. D.; Perakisa, C.; Tsimpanogiannisb, I. N.; Voutsasa, E. C. Thermodynamic modeling of the vapor−liquid equilibrium of the CO_2/H_2O mixture. *Fluid Phase Equilib.* **2009**, *284*, 56−63.

(98) Perfetti, E.; Thiery, R.; Dubessy, J. Equation of state taking into account dipolar interactions and association by hydrogen bonding: I— Modelling liquid−vapour equilibria in the $H_2O−H_2S$, $H_2O−CH_4$ and $H_2O−CO_2$ systems. *Chem. Geol.* **2008**, *251*, 50−57.

(99) Yunhai, S.; Honglai, L.; Kun, W.; Wende, X.; Ying, H. Measurements of isothermal vapor−liquid equilibrium of binary methanol/dimethyl carbonate system under pressure. *Fluid Phase Equilib.* **2005**, *234*, 1−10.

(100) Im, J.; Kim, M.; Lee, J.; Kim, H. Vapor−Liquid Equilibria of Binary Carbon Dioxide + Alkyl Carbonate Mixture Systems. *Korean J. Chem. Eng.* **2004**, *49*, 243−245.

(101) Lu, C.; Tian, Y.; Xu, W.; Li, D.; Zhu, R. High pressure phase equilibrium for the binary systems of carbon dioxide (1) + dimethyl carbonate (2) and carbon dioxide (1) + diethyl carbonate (2) at temperatures of 273 K, 283 K, and 293 K. *J. Chem. Thermodyn.* **2008**, *40*, 321−329.

(102) Bamberger, A.; Sieder, G.; Maurer, G. High-pressure (vapor−liquid) equilibrium in binary mixtures of (carbon dioxide−water or acetic acid) at temperatures from 313 to 353 K. *J. Supercrit. Fluids* **2000**, *17*, 97−110.

(103) Valtz, A.; Chapoy, A.; Coquelet, C.; Paricaud, P.; Richon, D. Vapour−liquid equilibria in the carbon dioxide−water system, measurement and modelling from 278.2 to 318.2 K. *Fluid Phase Equilib.* **2004**, *226*, 333−344.

(104) Yoon, J. H.; Chun, M. K.; Hong, W. H.; Lee, H. High-pressure phase equilibria for carbon dioxide−methanol−water system: Experimental data and critical evaluation of mixing rules. *Ind. Eng. Chem. Res.* **1993**, *32*, 2881−2887.